Extensive Laminin and Basement Membrane Accumulation Occurs at the Onset of Bleomycin-Induced Rodent Pulmonary Fibrosis

IRWIN I. SINGER, PhD, DOUGLAS W. KAWKA, BS, SUSAN M. McNALLY, BS, GEORGE J. EIERMANN, BS JOSEPH M. METZGER, MS, and LAURENCE B. PETERSON, PhD

From the Department of Experimental Pathology, Merck Sharp and Dohme Research Laboratories, Merck and Company, Inc., Rahway, New Jersey

The distribution of laminin was studied during pulmonary fibrosis induced in rodents by bleomycin sulfate. Large accumulations of laminin associated with basement membranes were seen in thickened lung interstitial spaces by immunofluorescence microscopy, starting at 7 days (32–75% increases) and persisting through 28 days (66–79% increase). By electron microscopy, these laminin concentrations were skeinlike masses of reduplicated basement membranes localized at the surface of alveolar capillary endothelial cells. Numerous macrophages were also associated with this basement membrane material. These findings suggest that bleomycin-induced damage to lung cells causes massive local accumulations of basement membranes, which might be involved in the expansion of the interstitial stroma by stimulating attachment and activation of certain inflammatory cells. (Am J Pathol 1986, 125:258–268)

PULMONARY FIBROSIS is a common morbid sequel following chronic lower respiratory tract inflammatory responses to a variety of etiologic agents.[1,2] These early stages of pneumonitis are characterized by the accumulation of numerous lymphocytes, plasma cells, and macrophages, together with scattered neutrophils.[3–5] Subsequently, increased numbers of fibroblasts secrete a collagenous extracellular matrix that progressively thickens the alveolar interstitium and severely compromises pulmonary function.[6–9] A single endotracheal dose of bleomycin sulfate induces a highly reproducible series of similar inflammatory and fibrotic pulmonary changes in rodents,[5,10] thus providing an excellent model of this disease. In this model, an acute inflammatory phase, characterized by a marked increase in the rate of collagen synthesis,[11] takes place from 6 to 8 days after bleomycin, whereas maximum interstitial collagen deposition occurs chronically from 30 to 60 days.[12] The acute cellular infiltrate consists mainly of macrophages and lymphocytes, whereas interstitial fibroblasts predominate in the chronic fibrotic phase.[5,12]

The connective tissue of normal lungs is composed of collagens I-V,[13,14] proteoglycans,[15,16] laminin (a component of alveolar and capillary basement membranes), and irregular quantities of fibronectin.[17–19] Although dramatic increases in the synthesis and accumulation of collagen,[5,11] proteoglycans,[15] and fibronectin[19] occur during pulmonary fibrosis, little is known about the distribution of laminin in the fibrotic lung.

Laminin (LN) is a 1 × 10^6-dalton molecular weight glycoprotein that is an integral component of basement membrane (BM).[20,21] This molecule mediates the substrate attachment and spreading of epithelial cells and fibroblasts *in vitro*,[22,23] and appears to play an important role in the chemotaxis and attachment of macrophages and neutrophils to inflammatory sites.[24,25] Because of these effects on cellular behavior, it is likely that laminin is involved in the pathogenesis of pulmonary fibrosis. Therefore, we have been investigating the ultrastructure of the lung extracellular matrix and the pulmonary distribution of LN in bleomycin-treated rodents.

Accepted for publication June 5, 1986.

Address reprint requests to Dr. Irwin I. Singer, Department of Experimental Pathology, Merck Sharp and Dohme Research Laboratories, P.O. Box 2000, Rahway, NJ 07065.

The fibrogenic response of rodents to bleomycin is genetically dependent. With collagen synthesis and deposition as a measure of the extent of fibrosis, CBA/J and C57Bl/6 mice developed significant pulmonary fibrosis, whereas Balb/c mice were poor responders; Fisher 344 rats were also high responders.[5,10,26] We studied high-responder strains of both mice and rats to determine whether putative changes in LN are of generalized occurrence during pulmonary fibrosis. Our results show a dramatic accumulation of LN-rich BM material within the fibrotic lungs of both species, suggesting that BM alterations play an important role in the development of fibrosing pulmonary lesions. A preliminary report of these observations was published elsewhere.[27]

Materials and Methods

Animals

Pulmonary fibrosis was induced by injecting 14 high-responder male CBA/J mice (28–30 g, 10–12 weeks old) through a tracheostomy with 0.015 units of bleomycin sulfate (Bristol Meyers, Syracuse, NY) in 0.05 ml of sterile saline and 10 male high-responder Fischer 344 rats (200–225 g, 12–14 weeks old) with 1.5 units of bleomycin in 0.3 ml of sterile saline, as previously described.[5,10] Control animals (10 mice and 4 rats) treated in a similar fashion received sterile saline. All animals were anesthetized by intraperitoneal injection of ketamine (Bristol Meyers) prior to intratracheal injection (mice, 3.7 mg; rats, 50 mg).

Fixation

The animals were sacrificed at 6–8 days (the acute inflammatory phase) or at 28 days (the chronic fibrotic phase) after bleomycin administration. Because pulmonary morphology is especially sensitive to the manner in which fixation is performed, we preserved these tissues by two different methods. Mice and rats were anesthetized by intraperitoneal injection of ketamine (mice, 7.5 mg; rats, 100 mg), and fixation was accomplished by either double perfusion or immersion. To obtain doubly perfused lungs, animals were cannulated through the right side of the heart, and the pulmonary vasculature was flushed with saline followed by fixative administered at a flow rate of 3–4 ml/min. As soon as vascular perfusion was initiated, the trachea was also cannulated and the pulmonary airways perfused with fixative under approximately 20 cm H_2O pressure. The lungs were subsequently excised and placed in fresh fixative. Lungs to be fixed by immersion were rapidly removed from anesthetized animals (which were exsanguinated by severing the vena cava) and immediately placed in fixative. Tissues intended for electron microscopy were rapidly macerated into 1-cu mm pieces. For light-microscopic studies of LN distribution, entire lung lobes were fixed with 3.5% formaldehyde (freshly generated from paraformaldehyde powder) in 0.1 M sucrose and 0.1 M Na-cacodylate (pH 7.2) containing 4.5 mM $CaCl_2$ for 24 hours. Tissues for electron microscopy were preserved with this formaldehyde fixative containing 2% glutaraldehyde for 24 hours, followed by washing and storage in cacodylate buffer containing 0.1% NaN_3 at 4 C. Electron-microscopic samples were obtained from 3 animals for both 7-day and 28-day treatment groups and from 2 animals in each control group.

Antibodies and Immunoconjugates

Rabbit antiserum monospecific for LN and purified LN isolated from Engelbreth-Holm-Swarm sarcoma BM by neutral salt extraction and DEAE cellulose chromatography, as previously described,[21] were generous gifts from Hynda K. Kleinman. This LN antiserum did not cross-react with other basement membrane antigens such as fibronectin, collagen IV, or entactin. The IgG fraction containing antibodies to LN was purified by 55% $(NH_4)_2SO_4$ precipitation and chromatography on protein A-Sepharose (Pharmacia, Inc., Piscataway, NJ). Fluorescein-conjugated affinity-purified goat anti-rabbit IgG for immunofluorescence microscopy was obtained commercially (Boehringer-Mannheim Biochemicals, Indianapolis, Ind). Unlabeled affinity-purified goat anti-rabbit IgG (Cappel Laboratories, West Chester, Pa) was conjugated to 20 nm diameter colloidal gold produced by Na-citrate reduction as previously described[28] for immunoelectron microscopy.

Immunofluorescence Microscopy

Entire lobes of 7-day or 28-day fibrotic lungs that were either perfusion- or immersion-fixed with 3.5% formaldehyde were embedded in paraffin; groups of 3 rats and 3 mice were preserved per time point, and 2 animals were used as controls for each species. Five-micron sections mounted on glass slides were dewaxed, rehydrated, and treated with pepsin in 0.01 N HCl as previously described for LN staining.[29] These lung sections were immunostained for LN by the following protocol with intervening washes in 0.1 M Tris HCl, pH 7.8: 1) nonimmune goat serum diluted 1/20 in Tris buffer, 2) monospecific anti-LN IgG (150 μg/ml), 3) affinity-purified FITC-goat anti-rabbit IgG diluted 1/25. Control sections were incubated in anti-LN IgG pretreated with a twofold excess (by weight) of purified LN (300 μg/ml for 16 hours; centrifuged at 15,000*g* for

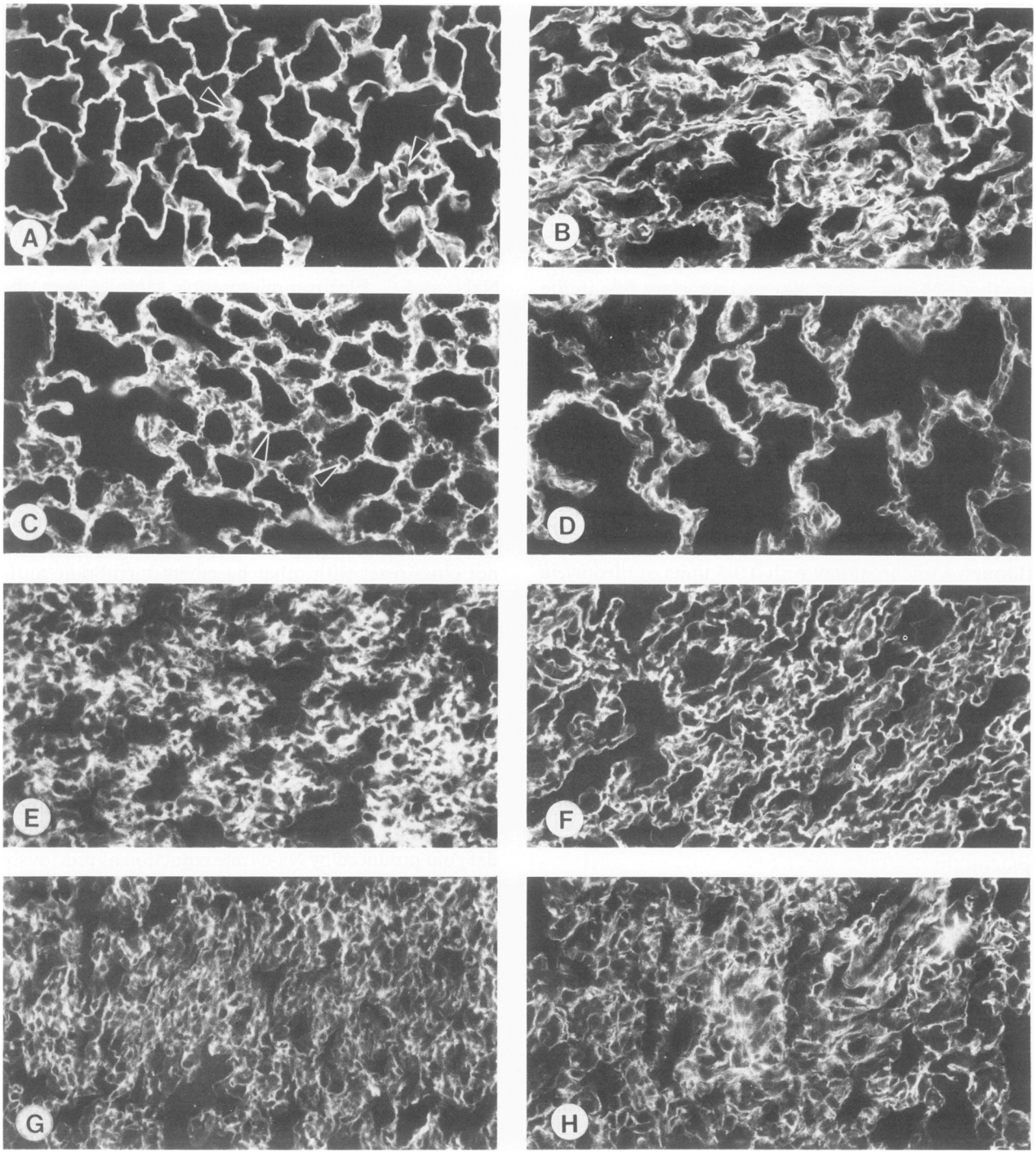

Figure 1—Immunofluorescence microscopic distribution of laminin in histologic sections of bleomycin-treated (fibrotic) and control mouse and rat lungs. **A** and **B** were prepared from doubly perfused lungs, and **C–H** are views of immersion-fixed tissues. (×275) **A**—Saline control CBA/J mouse. Alveolar basement membranes show intense continuous LN staining. A few blood vessels (*arrowheads*) are seen in the interalveolar spaces of this expanded specimen. **B**—CBA/J mouse. Many LN-stained basement membranes fill the thickened interstitial spaces of this expanded tissue fixed 8 days after 0.015 units bleomycin. **C**—Control CBA/J mouse lung fixed by immersion. All basement membranes are continously stained for LN. Numerous blood vessels (*arrowheads*) are present in the alveolar interstitium. **D**—Immersion-fixed control Fischer 344 rat lung is similar to the mouse lung in **C**. **E**—Fibrotic lesion in the immersion-fixed lung of a CBA/J mouse sacrificed 7 days after 0.015 units bleomycin. LN-stained basement membranes have an apparent matrixlike organization which occludes the air spaces. **F**—Extensive LN-stained basement membranes fill this fibrotic lesion of a Fischer 344 rat lung fixed via immersion 7 days after 1.5 units bleomycin. **G**—Matrjxlike appearance of LN-stained basement membranes persists in immersion-fixed fibrotic lung lesions of CBA/J mice given bleomycin 28 days previously. **H**—Persistent LN-positive basement membranes in a pulmonary fibrotic lesion of a Fischer 344 rat treated with 1.5 units bleomycin 28 days before immersion fixation.

15 minutes or in nonimmune rabbit IgG in Step 2 of this protocol. The stained sections were covered with 4% n-propyl gallate in glycerol[30] and photographed under standardized conditions (15-second exposures) with a Zeiss Photomicroscope III equipped with an Epifluorescence Condenser III RS, and ×16 (numerical aperture, 0.5) or ×40 (numerical aperture, 0.9) plan Neofluar objectives with the use of Ilford HP5 film processed at 1600 ASA. The relative quantities of LN staining in blind-coded lung photomicrographs were measured with an Image Technology Corporation (Deer Park, NY) Model 3000 image analysis system using a self-contained program operated in the density mode and a Nikon 55-mm lens (micro, 1:28).

Immunoelectron Microscopy

Tissue blocks of fibrotic lung lesions were preserved with the above formaldehyde/sucrose fixative containing 1% glutaraldehyde, cryoprotected with 2.3 M sucrose, quenched in liquid nitrogen-cooled Freon 22, and 0.1-μ ultrathin frozen sections were cut at −95 C by the Tokuyasu method[31] as previously described.[32] The ultrathin cryosections were mounted on grids and stained indirectly for LN by Steps 1 and 2 of the protocol for LN immunofluorescence microscopy, followed by affinity-purified goat anti-rabbit IgG–20 nm colloidal gold conjugate for 30 minutes at 25 C and postfixation in 2% glutaraldehyde in 0.1 M phosphate buffer, pH 7.2, for 5 minutes. Further section treatment with 2% OsO_4, 0.5% uranyl acetate in barbital buffer, and embedment in LR white acrylic resin (London Resin, London, UK) were performed as recently described.[33] Similar fibrotic lung tissues fixed with 3.5% formaldehyde in 0.1 M sucrose, 0.1 M cacodylate, 4.5 mM $CaCl_2$ containing 2% glutaraldehyde were processed solely for morphologic analysis. These blocks were treated with 1% OsO_4 and embedded in Epon. Silver-gray ultrathin sections were then stained with 2% uranyl acetate and lead citrate. Three to five blocks of lung tissue were studied for each bleomycin-treated and control animal sacrificed. Micrographs were taken with a JEOL 200 CX electron microscope using a specimen anticontamination device, a 40-μ objective lens aperture, a beam current of 5 μamp, and a vacuum of 10^{-7} mmHg.

Results

Distribution of Laminin

Immunofluorescence microscopy of LN in pepsin-treated paraffin sections of doubly-perfused saline-treated control CBA/J mouse lungs showed a continuous distribution of labeling on well-extended alveolar BM (Figure 1A). Immersion-fixed control specimens also had expanded alveoli, but showed numerous blood vessels in the alveolar interstitium (Figures 1C and D). Since the sequelae of bleomycin-induced pulmonary fibrosis have been classified into an acute inflammatory phase (6–8 days) and a chronic fibrotic period (about 28 days), we studied the distribution of LN at these intervals. Both immersion or perfusion-fixed CBA/J mouse and Fischer 344 rat lungs preserved 6–8 days after bleomycin administration exhibited massive concentrations of LN-positive BM which occluded the air spaces within these acute fibrotic lesions (Figure 1B, E, and F). Conspicuous accumulations of BM persisted through the chronic fibrotic phase for at least 28 days after treatment with bleomycin (Figures 1G and H). Control sections of normal or fibrotic lungs stained with nonimmune rabbit IgG or with LN antibodies pretreated with twofold excess purified LN showed very low levels of background labeling (see below).

Quantitation of Laminin Labeling

Quantitative measurements of LN-specific immunofluorescence staining were performed with an image

Table 1—Levels of Laminin Immunofluorescence in Bleomycin-Induced Pulmonary Fibrosis*

Species	Treatment	Mean % immunofluorescence	Ratio of bleomycin/saline	Data† compared
CBA/J mouse	Saline control, 7 days	48.8	–	–
CBA/J mouse	0.015 units bleomycin, 7 days	64.5	1.32	2 versus 1
CBA/J mouse	0.015 units bleomycin, 28 days	81.2	1.66	3 versus 1
F344 rat	Saline control, 7 days	46.5	–	–
F344 rat	1.5 units bleomycin, 7 days	81.6	1.75	5 versus 4
F344 rat	1.5 units bleomycin, 28 days	83.3	1.79	6 versus 4

* The mean percentage laminin-specific immunofluorescence staining was measured on photomicrographs (× 275) of lungs from groups of 3 bleomycin-treated animals fixed by immersion. All staining and photographic processing steps were standardized as indicated in Materials and Methods. The image analyzer was calibrated by adjusting the baseline for zero fluorescence with the use of a totally black (hence unlabeled) micrograph; the value for maximum fluorescence was obtained on a homogeneously white (thus fully labeled) micrograph. All measurements were expressed as a percentage of the maximum fluorescence.

† Confidence values were calculated with the Student unpaired *t* test. For each mean value, n = 10, SD < 4.3, and $P < 0.001$ for all comparisons listed.

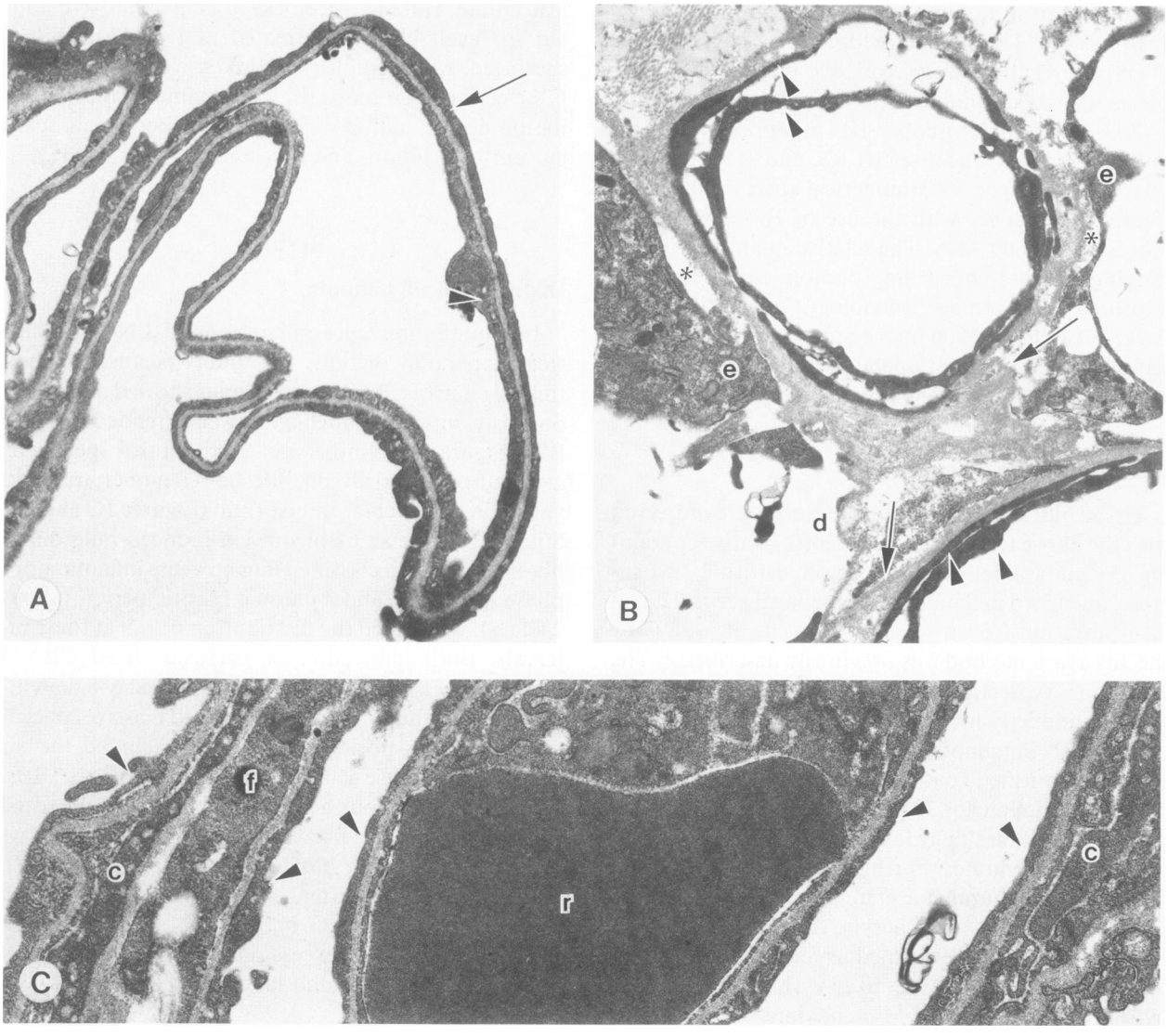

Figure 2—Electron micrographs of control and early fibrotic CBA/J mouse lungs fixed by double perfusion (**A** and **B**) or immersion (**C**). **A**—Saline-treated control lung preserved by vascular and tracheal perfusion. The pneumocytes (*arrow*) and capillary endothelial cells (*arrowhead*) are fully expanded and separated by a single thin basement membrane. (×20,800) **B**—Lung treated with 0.015 units bleomycin 8 days previously and fixed by double perfusion. The alveolar basement membranes are reduplicated (*arrows*) and greatly thickened. Several lamellae of endothelial cell cytoplasm (*arrowheads*) are concentrically arranged, the innermost layer separated from the basement membrane at several sites. The alveolar epithelium (*e*) is discontinuous (*d*), and clefts are present at the pneumocyte basement membrane (*asterisks*). (×12,650) **C**—Saline-treated control lung preserved by immersion fixation. Some collapsed capillaries (*c*) are present in the alveolar interstitium, and other capillaries are expanded with erythrocytes (*r*). Alveolar pneumocytes (*arrowheads*) and basement membranes are fully expanded and of normal thickness. *f*, interstitial fibroblast. (×21,120)

analyzer on photomicrographs of bleomycin-treated and control rodent lungs similar to those in Figure 1. These data, which represent the relative quantities of LN present in fibrotic lesions at various stages of pulmonary fibrosis, are shown in Table 1. Increases of 32%–75% of the LN labeling found in saline-treated control lungs were observed in the acute inflammatory phase at 7 days after bleomycin in both mice and rats. This increase in LN staining persisted through the chronic fibrotic phase at 28 days after bleomycin administration. Background fluorescence measured on fibrotic lung sections treated with nonimmune IgG in our staining protocol was less than 0.5% of the maximum LN immunofluorescence values.

Electron-Microscopic Examination of Pulmonary Fibrosis

To ensure that our fixation methods did not introduce substantial ultrastructural artifacts, fibrotic and control lungs were fixed for electron microscopy either by immersion or by double perfusion via the vascular and tracheal routes. Control tissues preserved by both

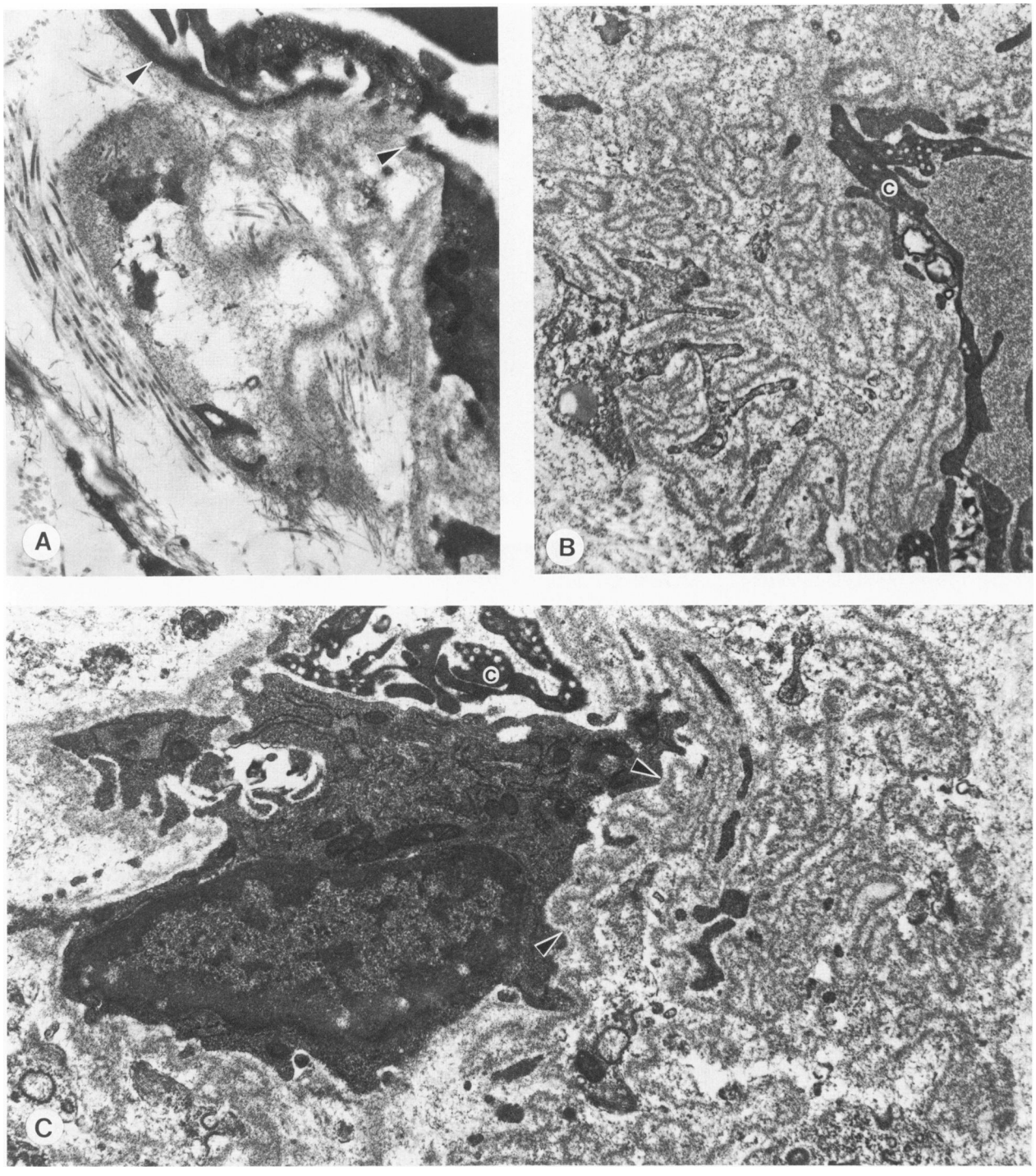

Figure 3—Early stages of bleomycin-induced lung fibrosis showing focal concentrations of extensively folded and reduplicated basement membranes in CBA/J mice and Fischer 344 rats. **A**—Reduplicated basement membranes are closely apposed to the capillary endothelium (*arrowheads*). Doubly perfused CBA/J mouse lung fixed 8 days after drug treatment (×19,000) **B**—Numerous skeinlike basement membranes fill the expanded interstitium adjacent to a capillary (*c*). Fischer 344 rat lung fixed by immersion 7 days after bleomycin administration. (×15,200). **C**—A macrophage is closely apposed (*arrowheads*) to the large mass of basement membranes which fills the pulmonary interstitium. *c*, capillary. Specimen similar to that shown in **B**. (×21,000)

methods exhibited expanded alveolar spaces and non-reduplicated basement membranes which were of normal thickness (40–100 nm) (Figure 2A and C). The alveolar capillaries of immersion-fixed controls were often filled with blood cells; or if empty, their lumens were collapsed (Figure 2C). In contrast, perfusion-fixed acutely inflamed lungs of animals given bleomycin 8 days previously exhibited dramatic changes in their interstitial basement membranes. Extensive reduplication and a two- to fourfold thickening of these basement

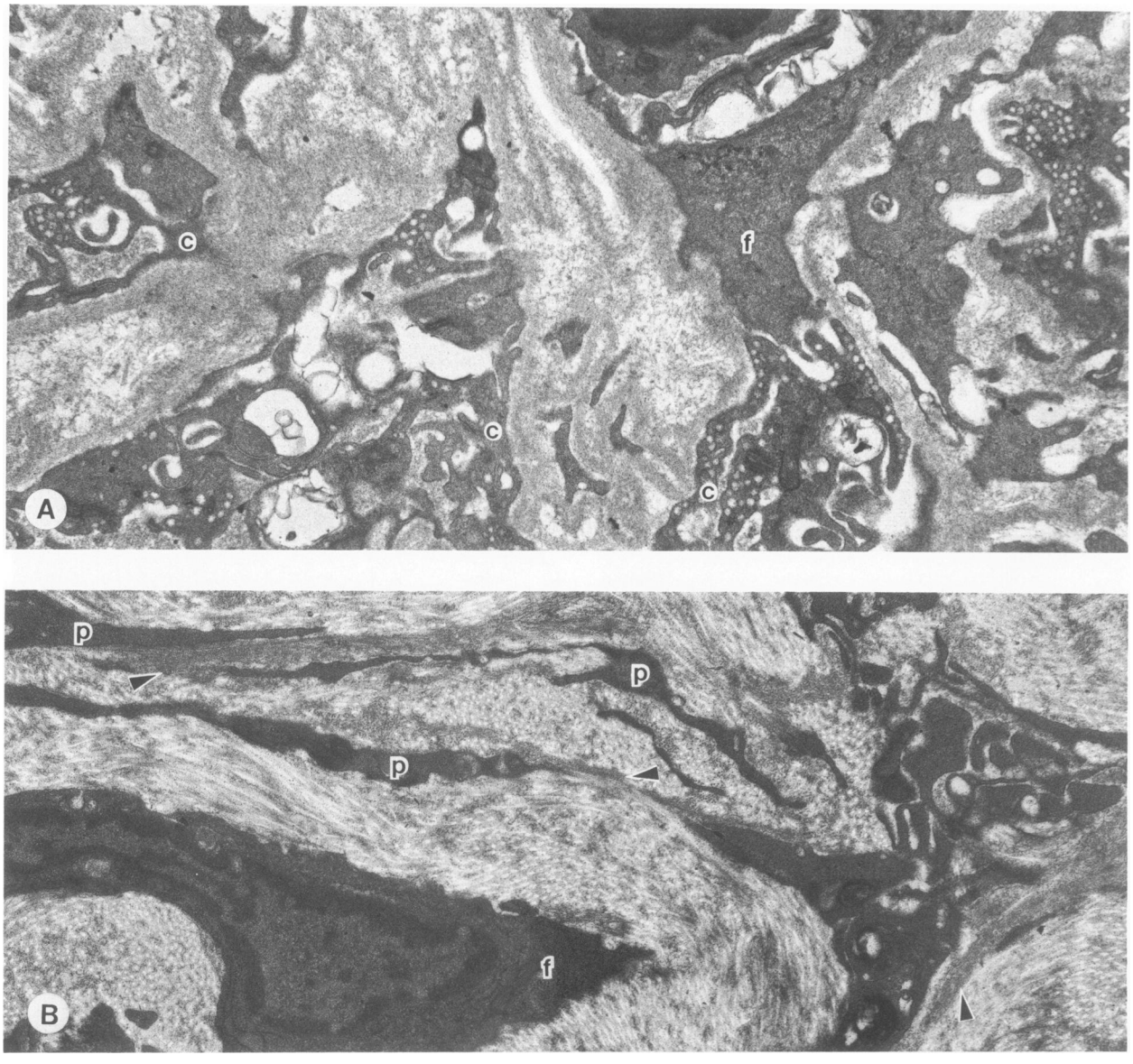

Figure 4—Later stages of pulmonary fibrosis 28 days after 0.015 units bleomycin in CBA/J mice. Immersion fixation. **A**—Thickened and reduplicated basement membranes persist at the periphery of alveolar capillaries (*c*). *f*, interstitial fibroblast. (× 14,200) **B**—Collagen fibers are very abundant and penetrated by attenuated cell processes (*p*) extending from interstitial fibroblasts (*f*). Some of these processes are in contact with persistent basement membrane material (*arrowheads*). (× 17,300)

membranes caused gross enlargement of the alveolar interstitial spaces (Figures 2B and 3A). These basement membrane alterations were present at both thin and thick (collagen containing) portions of the alveolar walls (Figure 2B). Necrotic changes such as gaps in the respiratory epithelium and edematous clefts between pneumocytes or endothelial cells and their basement membranes were also seen (Figures 2B and 3A). In addition, the capillary endothelia were frequently multilayered (Figure 2B). Very similar basement membrane alterations occurred in both CBA/J mouse and Fischer 344 rat lungs fixed via immersion 7 days after bleomycin treatment (Figure 3B and C). Large skeinlike masses of folded basement membrane material filled the interstitium adjacent to alveolar capillaries (Figure 3B); macrophages were often found closely apposed to these basement membranes (Figure 3C), whereas Type I pneumocytes were conspicuously absent from these regions. These basement membrane alterations were also found in fibrotic lungs preserved 28 days after bleomycin treatment (Figure 4A). Highly organized collagen bundles and attenuated fibroblasts associated with basement membrane material were also observed at this time (Figure 4B).

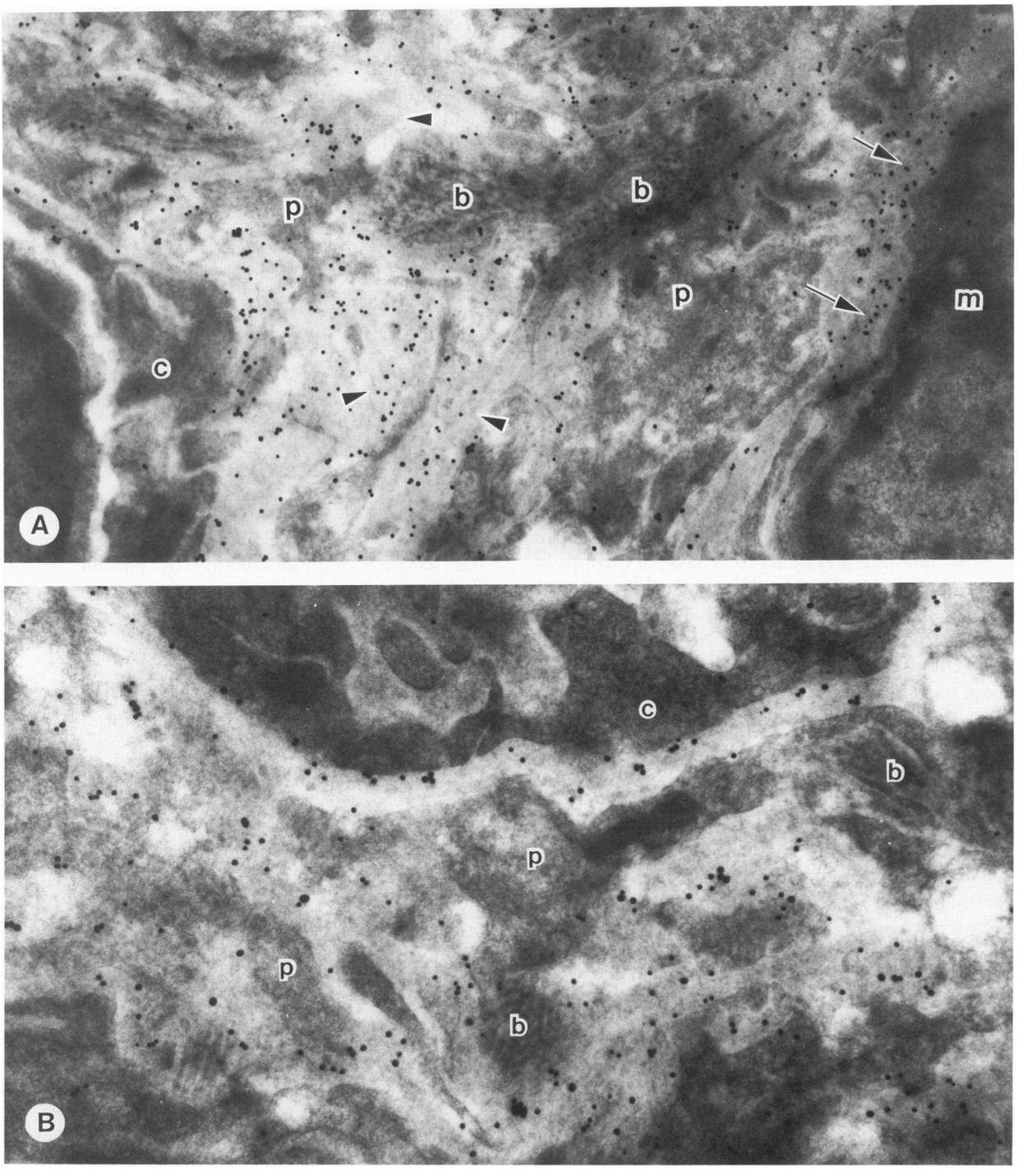

Figure 5—Immunoelectron micrographs of laminin in a Fischer 344 rat lung fibrotic lesion immersion-fixed 7 days after 1.5 units bleomycin. Ultrathin frozen sections were stained with rabbit anti-LN IgG, followed by goat anti-rabbit IgG conjugated to 20 nm colloidal gold. **A**—The expanded interstitium is filled with LN-positive skeinlike arrays of flocculent material (*arrowheads*) which resemble the convoluted basement membranes shown in Figure 3. A macrophage (*m*) similar to that in Figure 3C is closely apposed to LN-labeled basement membrane (*arrows*). This area also contains several collagen bundles (*b*) adjacent to fibroblast processes (*p*). The capillary (*c*) contains a leukocyte. (×21,000) **B**—A higher magnification view shows LN-positive basement membrane material surrounding the capillary endothelium (*c*). Bundles of collagen (*b*) and fibroblast processes (*p*) are unstained. (×40,000)

Immunoelectro-Microscopic Examination of Laminin

To correlate the elevated concentrations of laminin staining seen by immunofluorescence microscopy (Figures 1E and F) with the massive accumulation of basement membrane material observed in the acute phase of fibrosis (Figure 3), we performed immunoelectron microscopy on ultrathin cryosections of lung tissue fixed 7 days after bleomycin treatment. Using this

technique, basement membranes were not as condensed as in conventional Epon sections (compare Figures 3 and 5). Nevertheless, delicate feltlike basal laminae were found throughout the enlarged interstitium of 7-day fibrotic lungs at both thick and thin alveolar wall regions, and these structures were obviously LN-positive (Figure 5). LN-stained material was strikingly localized at the outer surfaces of macrophages (compare Figures 3C and 5A) and capillary endothelial cells. Interstitial collagen bundles, fibroblast processes, and capillary endothelial cells were not labeled. Sections stained with IgG obtained from unimmunized rabbits, or with anti-LN IgG preincubated with a twofold excess of purified LN, were completely unstained (not shown).

Discussion

Using immunofluorescence microscopy on histologic sections of mouse and rat lungs, we observed a conspicuous accumulation of laminin (increases of from 32% to 75%) associated with basement membranes in the early inflammatory phase (6–8 days) of bleomycin-induced pulmonary fibrosis. The chronic period of interstitial connective tissue accumulation (28 days) exhibited similar increases in laminin (66–79% increase). These changes probably reflect the large skein-like masses of reduplicated and thickened basement membrane which filled the expanded interstitium seen with electron microscopy. Such basement membrane aggregates were usually associated with capillary endothelial cells and alveolar macrophages; alveolar epithelial cells were conspicuously absent from these regions. We also showed that most of the flocculent material filling the expanded 7-day fibrotic lung interstitium is rich in laminin antigens with the use of immunoelectron microscopy. This striking concentration of basement membranes and laminin antigens during the early phases of bleomycin-induced lung fibrosis is probably not simply due to local tissue atelectasis caused by immersion fixation, because we observed similar basement membrane accumulation and reduplication in expanded lungs at both the light- and electron-microscopic levels. Accompanying this basement membrane accumulation, we saw edematous spaces beneath both alveolar epithelial and endothelial cells and necrotic regions in the epithelium (indicated by gaps between the pneumocytes). These alterations are probably caused by the extremely high sensitivity of lung cells to bleomycin-induced DNA damage relative to other tissues.[34] Similar pathologic changes were previously reported for bleomycin-treated rodents, and for radiation-induced pulmonary fibrosis,[35–37] but basement membrane reduplication was not observed in these studies. However, recent observations on specimens from patients with active pulmonary fibrosis do indeed report BM reduplication associated with lung capillaries.[19] (Interestingly, these multilayered basement membranes are also rich in fibronectin.[19]) Furthermore, subsequent to the completion of our experiments, Vaccaro et al reported that pleated pulmonary epithelial cell basement membranes accumulated in the alveolar interstitium at 6 days and were reduplicated by 30 days after bleomycin administration to hamsters.[50] Thus, BM reduplication may be a common feature of pulmonary fibrosis in several rodent species and in man.

We used image analysis to quantify the accumulation of LN in immunofluorescence micrographs of fibrotic lungs and measured substantial increases in LN staining in the acute and fibrotic phases of lung fibrosis. This method may be subject to some imprecision because of variations in lung inflation and section thickness. However, we found that increases in LN staining caused by immersion fixation (relative to perfused specimens) were minor, compared with the large LN accumulation measured after bleomycin treatment. Variations in section thickness were similarly inconsequential, because immunolabeling of paraffin sections mainly occurs at the section surface (this method requires pepsin treatment to unmask the superficial LN antigens). We therefore believe that our image analysis measurements are valid.

Basement membrane reduplication has been reported in a number of other pathologic conditions such as rheumatoid arthritis,[38] gliosarcomas,[39] melanomas metastatic to the brain,[40] diabetic microangiopathy,[41] and nephropathies induced by freezing or irradiation.[42,43] In most of these cases, basement membrane reduplication is closely associated with vascular proliferation, in which multiple layers of basement membrane are synthesized by successive generations of dying and proliferating endothelial cells. Connective tissue accumulation and scar formation usually accompanies these events. We believe that a similar process occurs in bleomycin-induced pulmonary fibrosis in rodents. The damage to both the alveolar epithelium and endothelium due to bleomycin treatment evidently causes these cells to separate from their basement membranes (causing, eg, formation of edematous clefts). This separation might induce multiple rounds of basement membrane synthesis, which could account for the basement membrane accumulation that we observed. Alternatively, the alveolar epithelial cell destruction that we found might also free up preexisting basement membranes that could accumulate in the alveolar interstitium. Regardless of their origin, these masses of pleated basement membranes do not support normal attachment of the dividing Type II pneumocytes. This abnormality could be one of the causes of increased interstitial matrix synthesis (ie, collagen Types I and III, fibronectin, proteoglycan) characteristic of pulmonary

fibrosis, because basement membrane malformation usually results in scars, rather than tissue reconstruction, in healing injuries.[41]

Because bleomycin-mediated pulmonary fibrosis is a two-component model exhibiting acute inflammation and chronic fibrosis, it is possible that the massive basement membrane reduplication that we observed is associated primarily with either inflammation or fibrosis. Therefore, we have also studied mouse lungs injected with the killed bacille Calmette–Guerin strain of *Mycobacterium bovis*,[44] which exhibit extensive granulomatous inflammation without substantial fibrosis.[45] Although some basement membrane thickening was found in the 28-day granulomas, we did not observe BM reduplication in any of our granulomatous lung specimens (unpublished observations). We therefore speculate that abnormal basement membrane accumulation plays some role in stimulating mesenchymal proliferation in the bleomycin fibrotic lung model. This hypothesis is supported by the recent experiments of McArdle et al,[40] who report that basement membrane redevelopment is positively correlated with the presence of mesenchymal tissue surrounding metastatic brain carcinomas.

The appearance of greatly expanded basement membrane material during early bleomycin-induced pulmonary fibrosis might function in the selective attachment of certain inflammatory cells and lymphocytes which are apparently critical to the development of these lung lesions. Schrier et al have shown that bleomycin treatment of athymic nude mice results in only partial expression of lung fibrosis[46] and that this effect is modulated by suppressor T cells in euthymic mice.[26] In addition, the numerous macrophages which were associated with reduplicated basement membranes might stimulate lung fibroblasts to synthesize extracellular matrix material. Laminin has also been detected at the surfaces of peritoneal macrophages[25] and neutrophils,[24] where it mediates their attachment to basement membranes via collagen Type IV.[23] Based on these findings, we hypothesize that the basement membrane masses which develop in fibrotic lung tissue might be a substrate for the attachment and activation of T cells and macrophages that are required for full expression of bleomycin-induced pulmonary fibrosis. Indeed, activated macrophages secrete interleukin I-like factors which stimulate the synthesis of interstitial collagen by fibroblasts,[47] basement membrane collagen by mammary epithelial cells,[48] and glycosaminoglycans by vascular endothelial cells.[49] We are currently investigating this hypothesis.

References

1. Crystal RG, Gadek JE, Ferrans VJ, Fulmer JD, Line BR, Hunninghake GW: Interstitial lung disease-current concepts of pathogenesis, staging, and therapy. Am J Med 1981, 70:542–568
2. Phan SH: Fibrotic mechanisms in lung diseases. In: Ward PA, ed, Immunology of Inflammation. New York, Elsevier, 1983, pp 121–161
3. Luna, MA, Bedrosian CWM, Lichtiger B, Salem PA: Interstitial pneumonitis associated with bleomycin therapy. Am J Clin Pathol 1972, 58:501–510
4. Schoenberger CI, Rennard SI, Bitterman PB, Fukuda Y, Ferrans VJ, Crystal RG: Paraquat-induced pulmonary fibrosis: Role of the alveolitis in modulating the development of fibrosis. Am Rev Respir Dis 1984, 129:168–173
5. Thrall RS, McCormick JR, Jack RM, McReynolds RA, Ward PA: Bleomycin-induced pulmonary fibrosis in the rat. Am J Pathol 1979, 95:117–130
6. Crystal RG, Fulmer JD, Roberts WC, Moss ML, Line BR, Reynolds HY: Idiopathic pulmonary fibrosis-clinical histologic, radiographic, physiologic, scintigraphic, cytologic, and biochemical aspects. Ann Intern Med 1976, 85:769–788
7. Kissler W: Formal genesis of pulmonary fibrosis: experimental investigations. Curr Top Pathol 1983, 73: 207–231
8. Phan SH, Thrall RS, Ward PA: Bleomycin-induced pulmonary fibrosis in rats: Biochemical demonstration of increased rate of collagen synthesis. Am Rev Respir Dis 1980, 121:501–506
9. Scadding JB, Hinson KFW: Diffuse fibrosing alveolitis: Correlation of histology at biopsy with prognosis. Thorax 1967, 22:291–304
10. Schrier DJ, Kunkel RG, Phan SH: The role of strain variation in murine bleomycin-induced pulmonary fibrosis. Am Rev Respir Dis 1983, 127:63–66
11. Clark JG, Overton JE, Marino BA, Uitto J, Starcher BC: Collagen biosynthesis in bleomycin-induced pulmonary fibrosis in hamsters. J Lab Clin Med 1980, 96:943–953
12. Snider GL, Hayes JA, Korthy AL: Chronic interstitial pulmonary fibrosis produced in hamsters by endotracheal bleomycin. Am Rev Respir Dis 1978, 117:1099–1108
13. Bradley K, McConnell-Breul S, Crystal RG: Lung collagen heterogeneity. Proc Natl Acad Sci USA 1974, 71: 2828–2832
14. Hance AJ, Bradley K, Crystal RG: Lung collagen heterogeneity: Synthesis of type I and type III collagen by rabbit and human lung cells in culture. J Clin Invest 1976, 57:102–111
15. Cantor JO, Osman M, Cerrata JM, Mandl I, Turino GM: Glycosaminoglycan synthesis in explants derived from bleomycin treated fibrotic hamster lungs. Proc Soc Exp Biol Med 1983, 173:362–366
16. Vaccaro CA, Brody JS: Ultrastructural localization and characterization of proteoglycans in the pulmonary alveolus. Am Rev Respir Dis 1979, 120:901–910
17. Gil J, Martinez-Hernandez A: The connective tissue of the rat lung: electron immunohistochemical studies. J Histochem Cytochem 1984, 32:230–238
18. Stenman S, Vaheri A: Distribution of a major connective tissue protein, fibronectin, in normal human tissues. J Exp Med 1978, 147:1054–1064
19. Torikata C, Villiger B, Kuhn C, III, McDonald JA: Ultrastructural distribution of fibronectin in normal and fibrotic human lung. Lab Invest 1985, 52:399–408
20. Kleinman HK, McGarvey ML, Hassell JR, Martin GR, Baron van Evercooren A, Dubois-Dalcq M: The role of laminin in basement membranes and in the growth, adhesion, and differentiation of cells, The Role of Extracellular Matrix in Development. Edited by RL Trelstad. New York, Alan R. Liss, 1984, pp 123–143
21. Timpl R, Rohde H, Robey PG, Rennard SI, Foidart J-M, Martin GR: Laminin-A glycoprotein from basement membranes. J Biol Chem 1979, 254:9933–9937
22. Couchman JR, Hook M, Rees DA, Timpl R: Adhesion,

growth, and matrix production by fibroblasts on laminin substrates. J Cell Biol 1983, 96:177–183
23. Terranova VP, Rohrbach DH, Martin GR: Role of laminin in the attachment of PAM 212 (epithelial) cells to basement membrane collagen. Cell 1980, 22:719–726
24. Terranova VP, Liotta LA, Vasanthakumar G, Thorgeirsson U, Siegal GP, Schiffmann E: Role of laminin in the adherence and chemotaxis of neutrophils. Fed Proc 1983, 42:2851–2852
25. Wicha MS, Huard TK: Macrophages express cell surface laminin. Exp Cell Res 1983, 143:475–479
26. Schrier DJ, Phan SH: Modulation of bleomycin-induced pulmonary fibrosis in the BALB/c mouse by cyclophosphamide-sensitive T cells. Am J Pathol 1984, 116: 270–278
27. Singer II, Kawka DW, Kazazis DM, Eiermann GJ: Laminin forms a prominent extracellular matrix at the onset of pulmonary fibrosis. J Cell Biol 1974, 99:75a
28. De Mey J: Colloidal gold probes in immunocytochemistry. In: Polak, JM, Van Noorden S, eds. Immunocytochemistry. Boston, Wright-PSG, 1983, pp 82–112
29. Kirkpatrick P, D'Ardenne AJ: Effects of fixation and enzymatic digestion on the immunohistochemical demonstration of laminin and fibronectin in paraffin embedded tissue. J Clin Pathol 1984, 34:639–644
30. Giloh H, Sedat JW: Fluorescence microscopy: reduced photobleaching of rhodamine and fluorescein protein conjugates by n-propyl gallate. Science 1982, 217: 1252–1255
31. Tokuyasu KT: Immunocytochemistry on ultrathin frozen sections. Histochem J 1980, 12:381–403
32. Singer II, Kawka DW, Kazazis DM, Clark RA: *In vivo* co-distribution of fibronectin and actin fibers in granulation tissue: Immunofluorescence of the fibronexus at the myofibroblast surface. J Cell Biol 1984, 98:2091–2105
33. Keller GA, Tokuyasu KT, Dutton AH, Singer SJ: An improved procedure for immunoelectron microscopy: Ultrathin plastic embedding of immunolabeled ultrathin frozen sections. Proc Natl Acad Sci USA 1984, 81:5744–5747
34. Lazo JS, Humphreys CJ: Lack of metabolism as the biochemical basis of bleomycin-induced pulmonary toxicity. Proc Natl Acad Sci USA 1983, 80:3064–3068
35. Adamson IYR: Drug induced pulmonary fibrosis. Environ Health Perspect 1984, 55:25–36
36. Adamson IYR, Bowden DH: The pathogenesis of bleomycin-induced pulmonary fibrosis in mice. Am J Pathol 1974, 77:185–190
37. Adamson IYR, Bowden DH: Endothelial injury and repair in radiation-induced pulmonary fibrosis. Am J Pathol 1983, 112:224–230
38. Scott DL, Salmon M, Morris CJ, Wainwright AC, Walton KW: Laminin and vascular proliferation in rheumatoid arthritis. Ann Rheum Dis 1984, 43:551–555
39. Schiffer D, Giordana MT, Mauro A, Migheli A: GFAP, FVIII/RAg, laminin, and fibronectin in gliosarcomas: An immunohistochemical study. Acta Neuropathol 1984, 63:108–116
40. McArdle JP, Muller HK, Roff BT, Murphy WH: Basal lamina redevelopment in tumours metastatic to brain: an immunoperoxidase study using an antibody to type-IV collagen. Int J Cancer 1984, 34:633–638
41. Vracko R: Basal lamina scaffold-anatomy and significance for maintenance of orderly tissue structure. Am J Pathol 1974, 77:313–338
42. Pierce GB, Nakane PK: Basement membranes: Synthesis and deposition in response to cellular injury. Lab Invest 1969, 21:27–41
43. Thorning D, Vracko R: Renal glomerular basal lamina scaffold: Embryologic development, anatomy, and role in cellular reconstruction of rat glomeruli injured by freezing and thawing. Lab Invest 1977, 37:105–119
44. Allen EM, Moore VL, Stevens JO: Strain variation in BCG-induced chronic inflammation in mice: I. Basic model and possible genetic control by non-H-2 genes. J Immunol 1977, 119:343–347
45. Adams DO: The structure of mononuclear phagocytes differentiating *in vivo*. Am J Pathol 1974, 76:17–48
46. Schrier DJ, Phan SH, McGarry BM: The effects of the nude (nu/nu) mutation on bleomycin-induced pulmonary fibrosis. Am Rev Respir Dis 1983, 127:614–617
47. Vaes, G: Macrophage-secretory products and connective tissue remodeling: role of macrophage enzymes and of "matrix regulatory monokines." Dev Cell Biol 1984, 1:1–80
48. Matsushima K, Bano M, Kidwell WR, Oppenheim JJ: Interleukin I increases collagen type IV production by murine mammary epithelial cells. J Immunol 1985, 134:904–909
49. Montesano R, Mossaz A, Ryser JE, Orci L, Vassalli P: Leukocyte interleukins induce cultured endothelial cells to produce a highly organized, glycosaminoglycan-rich pericellular matrix. J Cell Biol 1984, 99:1706–1715
50. Vaccaro CA, Brody JS, Snider GL: Alveolar wall basement membranes in bleomycin-induced pulmonary fibrosis. Am Rev Respir Dis 1985, 132:905–912

Acknowledgments

The authors thank Dr. Vernon L. Moore for reviewing this paper and for constant intellectual stimulation as well as support of this work. We are also grateful to Dr. John A. McDonald for helpful discussions and for providing a preprint of recent experiments and to Dr. Hynda K. Kleinman for her generous gifts of purified LN and anti-LN antibodies. We also thank Karl H. Nollstadt for affinity purification of antibodies and Eileen M. Miller for typing the manuscript.